First, E. A., & Taylor, S. S. (1988) *J. Biol. Chem. 263*, 5170–5175.
Hofmann, F., Beavo, J. A., Bechtel, P. J., & Krebs, E. G. (1975) *J. Biol. Chem. 250*, 7795–7801.
Hoppe, J., Marutzky, R., Freist, W., & Wagner, K. G. (1977) *Eur. J. Biochem. 80*, 369–372.
Hoppe, J., Freist, W., Marutzky, R., & Shaltiel, S. (1978) *Eur. J. Biochem. 90*, 427–432.
Laemmli, U. K. (1970) *Nature (London) 227*, 680–685.
Nelson, N. C., & Taylor, S. S. (1981) *J. Biol. Chem. 256*, 3743–3750.
Øgreid, D., & Døskeland, S. O. (1981) *FEBS Lett. 129*, 287–292.
Øgreid, D., & Døskeland, S. O. (1983) *Biochemistry 22*, 1686–1696.
Øgreid, D., Døskeland, S. O., & Miller, J. P. (1983) *J. Biol. Chem. 258*, 1041–1049.
Rangel-Aldao, R., & Rosen, O. M. (1976) *J. Biol. Chem. 251*, 7526–7529.
Ringheim, G. E., & Taylor, S. S. (1990) *J. Biol. Chem. 265*, 4800–4808.
Robinson, G. A., Butcher, R. W., & Sutherland, E. W. (1971) *Cyclic AMP*, Academic Press, Inc., New York.
Rosen, O. M., & Erlichman, J. (1975) *J. Biol. Chem. 250*, 7788–7794.
Rothermel, J. D., & Botelho, L. H. P. (1988) *Biochem. J. 251*, 757–762.
Saraswat, L. D., Filutowics, M., & Taylor, S. S. (1986) *J. Biol. Chem. 261*, 11091–11096.
Saraswat, L. D., Ringheim, G. A., Bubis, J., & Taylor, S. S. (1988) *J. Biol. Chem. 263*, 18241–18246.
Takio, K., Walsh, K. A., Neurath, H., Smith, S. B., Krebs, E. G., & Titani, K. (1980) *FEBS Lett. 114*, 83–88.
Takio, K., Smith, S. B., Krebs, E. G., Walsh, K. A., & Titani, K. (1984) *Biochemistry 23*, 4200–4206.
Taylor, S. S., Kerlavage, A. R., Zoller, M. J., Nelson, N. C., & Potter, R. L. (1981) *Cold Spring Harbor Symp. Protein Phosphorylation. Book A 8*, 3–18.
Taylor, S. S., Buechler, J. A., & Yonemoto, Y. (1990) *Annu. Rev. Biochem. 59*, 971–1005.
Titani, K., Sasagawa, T., Ericsson, L. H., Kumar, S., Smith, S. B., Krebs, E. G., & Walsh, K. A. (1984) *Biochemistry 23*, 4193–4199.
Weber, I. T., Takio, K., Titani, K., & Steitz, T. A. (1982) *Proc. Natl. Acad. Sci. U.S.A. 79*, 7679–7683.
Weber, I. T., Steitz, T. A., Bubis, J., & Taylor, S. S. (1987) *Biochemistry 26*, 343–351.
Zoller, M. J., & Taylor, S. S. (1979) *J. Biol. Chem. 254*, 8363–8368.

Pulsed EPR Analysis of Tartrate Dehydrogenase Active-Site Complexes†

Peter A. Tipton* and Jack Peisach
Department of Molecular Pharmacology, Albert Einstein College of Medicine, Bronx, New York 10461
Received July 10, 1990; Revised Manuscript Received October 8, 1990

ABSTRACT: Mn^{2+}·tartrate dehydrogenase·substrate complexes have been examined by electron spin echo envelope modulation spectroscopy. The occurrence of dipolar interactions between Mn^{2+} and ^2H on [^2H]pyruvate and [4-^2H]NAD(H) confirms that Mn^{2+} binds at the enzyme active site. The ^2H signal arising from labeled pyruvate was lost if the sample was incubated at room temperature, indicating that the enzyme catalyzes exchange between the pyruvate methyl protons and solvent protons. Mn–^{133}Cs dipolar coupling was also observed, which suggests that the monovalent cation cofactor also binds in the active site. The tartrate analogue oxalate was observed to have a significant effect on the binding of NAD(H). Oxalate appears to constrain the binding of NAD(H) so that the nicotinamide portion of the cofactor is held in close proximity to Mn^{2+}. Spectra of enzyme complexes prepared with (*R*)-[4-^2H]NADH showed a more intense ^2H signal than analogous complexes prepared with (*S*)-[4-^2H]NADH, demonstrating that the *pro-R* position of NADH is closer to Mn^{2+} than the *pro-S* position and suggesting that tartrate dehydrogenase is an A-side-specific dehydrogenase. Oxalate also affected Cs^+ binding; the intensity of the ^{133}Cs signal increased in the presence of oxalate, which suggests that oxalate facilitates binding of Cs^+ to the active site or that Cs^+ binds closer to Mn^{2+} when oxalate is present. In addition to signals from substrates, electron spin echo envelope modulation spectra revealed ^{14}N signals that arose from coordination to Mn^{2+} by nitrogen-containing ligands from the protein; however, the identity of this ligand or ligands remains obscure.

Tartrate dehydrogenase is induced in *Pseudomonas putida* by growth on (+)-tartrate as the sole carbon source and catalyzes the first step in the catabolism of tartrate (Kohn & Jakoby, 1968), the NAD^+-dependent oxidation of (+)-tartrate to oxaloglycolate. TDH[1] has also been found to catalyze two other reactions, the oxidative decarboxylation of D-malate and the net nonoxidative decarboxylation of *meso*-tartrate (Tipton & Peisach, 1990). All these reactions also require Mn^{2+} and K^+ as cofactors. There are a variety of mechanisms through which Mn^{2+} potentially could participate in these reactions, for example, by lowering the p*K* of the hydroxyl group at the carbon center being oxidized, by facilitating decarboxylation

† Supported by NIH Grants GM 40168 and RR 02583. P.A.T. was supported by NIH Postdoctoral Fellowship GM 12081.
* Address correspondence to this author at his present address: Department of Biochemistry, M121 Medical Sciences Building, University of Missouri—Columbia, Columbia, MO 65212.

[1] Abbreviations: TDH, tartrate dehydrogenase; EPR, electron paramagnetic resonance; ESEEM, electron spin echo envelope modulation; ESE, electron spin echo; TEA, triethanolamine; HEPES, *N*-(2-hydroxyethyl)piperazine-*N*′-2-ethanesulfonic acid; Tris, tris(hydroxymethyl)aminomethane; DTT, dithiothreitol.

0006-2960/91/0430-739$02.50/0

of the putative β-keto acid intermediates in the D-malate and *meso*-tartrate reactions, or by serving to correctly orient the substrates in the active site. K^+ may have similar functions or may be required to neutralize charge on the substrates.

We have investigated the environment of Mn^{2+} bound to TDH using the pulsed EPR technique electron spin echo envelope modulation spectroscopy (Mims & Peisach, 1981). In this way, we have detected weak magnetic interactions between Mn^{2+} and the other species bound at the active site. These data demonstrate that Mn^{2+}, the substrates, and the alkali metal ion cofactor all bind within several angstroms of each other and suggest a possible arrangement of the reactants in the active site.

ESEEM spectra also revealed ^{14}N interactions with Mn^{2+}, which must arise from nitrogen–ligand coordination to the metal by the protein. Model studies aimed at distinguishing between different potential ligands such as the ε-amine of lysine and the imine nitrogen of imidazole from histidine demonstrated, however, that Mn·amine and Mn·imine complexes give rise to similar ESEEM spectra.

Materials and Methods

TDH was isolated from *P. putida* ATCC strain 17642 by the following modifications of the procedure described earlier (Tipton & Peisach, 1990). The purification scheme through the heat treatment step remained the same; however, anion-exchange chromatography was performed on a 3.0 × 30 cm column of Pharmacia Q Sepharose Fast Flow resin. TDH was eluted with a 2-L gradient from 0 to 1 M NaCl in 15 mM TEA buffer, pH 7.8, containing 1 mM DTT. Active fractions were pooled and concentrated to 10 mL by ultrafiltration with an Amicon PM30 membrane. The concentrated protein was applied to a 3.0 × 95 cm column of LKB AcA 44 gel-filtration resin equilibrated in the same TEA buffer, containing 0.1 M NaCl. The column was eluted at 0.5 mL/min, and those fractions containing TDH were concentrated by ultrafiltration. The protein was then applied to a Pharmacia Mono Q HR 10/10 column and was eluted at 2.0 mL/min with a 0.24-L gradient from 0 to 1 M NaCl in the same TEA buffer as above. Active fractions were concentrated, desalted into 100 mM K^+HEPES buffer, pH 8.0, containing 1 mM DTT by using a 1.2 × 28 cm Sephadex G-25 column, reconcentrated, and stored at 4 °C in the presence of 10% glycerol. TDH prepared in this way routinely had a specific activity of 1.0 ± 0.1 unit/mg (Tipton & Peisach, 1990) and was homogeneous as determined by SDS–polyacrylamide gel electrophoresis followed by Coomassie staining.

Interpretation of ESEEM spectra of TDH complexes required that all the Mn^{2+} in the sample was protein-bound. Appropriate conditions were determined by continuous wave EPR titration, using a Varian E112 spectrometer operating at 9.1 GHz. Samples (30 μL) were contained in 1.0-mm i.d. quartz capillaries, and spectra were acquired at room temperature. TDH was titrated into solutions containing 150 μM Mn^{2+} and other reaction components. Binding of Mn^{2+} to TDH was detected by the diminution of the free Mn^{2+} spectrum (Cohn & Townsend, 1954). The concentration of free Mn^{2+} was judged to be negligible when increasing the concentration of TDH had no effect on the amplitude of the EPR signal. No attempt was made to calculate the Mn^{2+} dissociation constant from these data; however, steady-state kinetic studies (Tipton & Peisach, 1990) have demonstrated that Mn^{2+}, which binds to the enzyme prior to the other substrates, has a dissociation constant of about 60 μM. The value of K_d appears to be relatively insensitive to whether (+)-tartrate or D-malate is the substrate. Samples for ESEEM analysis of TDH were prepared in a total volume of 105 μL and contained Mn^{2+} and TDH at the concentrations determined by the EPR titration experiments. Concentrations of TDH stock solutions were determined by the Bradford protein assay (Bradford, 1976) with the Bio-Rad protein assay reagent and bovine serum albumin as the standard.

TDH complexes prepared for ESEEM analysis contained 10% glycerol. Unless otherwise stated, all reagents were used as the free acid or potassium salt, and the pH was adjusted with HCl or KOH. Approximately 5 min was required to prepare the sample and load it into the transmission cavity (Mims, 1974), prior to freezing.

Mn^{2+} model complexes with urocanate, histidine, and aspartate were prepared from stock solutions that had been sparged with N_2, and all manipulations were performed under N_2. The stock solutions were unbuffered; the urocanate solution was adjusted to pH 7.3, and the histidine solution, to pH 7.0. Because MnO_2 is formed as an insoluble precipitate at high pH, the aspartate stock solution was adjusted to pH 7.7, well below the α-NH_2 pK of 9.8. ESEEM samples contained 50% ethylene glycol to preserve magnetic dilution in the frozen solution. The Mn·aspartate sample contained 0.5 mM Mn^{2+} and 45 mM aspartate, the Mn·histidine sample contained 0.5 mM Mn^{2+} and 45 mM histidine, and the Mn·urocanate sample consisted of 0.5 mM Mn^{2+} and 22.5 mM urocanate.

ESE modulation envelopes of protein samples were obtained by using a stripline transmission cavity identical with that described by Mims (1974); model complexes were contained in standard 4-mm EPR tubes and were studied by using a reflection cavity (Britt & Klein, 1987) that employs a folded stripline as the resonant element (Lin et al., 1985). Data were collected by using a home-built pulsed EPR spectrometer (McCracken et al., 1987) operating at X-band. The envelope modulation patterns were acquired using a three-pulse stimulated echo sequence (Peisach et al., 1979) and consisted of 1024 data points for which each point was the average of 75 measurements of the echo amplitude at that value of $T + \tau$, where T is the delay between the second and third microwave pulses and τ is the delay between the first and second pulses. The repetition rate between pulse cycles was 213 Hz, and T was increased in 5-ns increments with each cycle; sample temperature was maintained at 1.8 K by using a helium immersion dewar under reduced pressure. Other experimental parameters are given in the appropriate figure legends. Modulation envelope data were analyzed by using the dead-time reconstruction procedure of Mims (1984), followed by Fourier transformation.

[$^2H_3$]Pyruvate was prepared as described by Attwood et al. (1986), and labeling was judged to be essentially complete on the basis of ^1H NMR analysis. (*S*)-[4-^2H]NADH was prepared by reducing NAD^+ with *Leuconostoc mesenteroides* glucose-6-phosphate dehydrogenase in the presence of [1-^2H]glucose 6-phosphate in 20 mM HEPES buffer pH 7.8. [4-^2H]NAD^+ was prepared by oxidizing (*S*)-[4-^2H]NADH with lactate dehydrogenase. [4-^2H]NAD^+ was reduced by *L. mesenteroides* glucose-6-phosphate dehydrogenase in the presence of protioglucose 6-phosphate to yield (*R*)-[4-^2H]-NADH. Reduced pyridine nucleotides were applied to a DEAE-Sephadex A-25 column and eluted with a gradient of 0–5 M $(NH_4)_2CO_3$. Oxidized pyridine nucleotide was purified on a column of Dowex-1 in the formate form; elution was accomplished with a gradient of 0–1.5 M formic acid.

Results

Tartrate Dehydrogenase Complexes. ESEEM spectra of

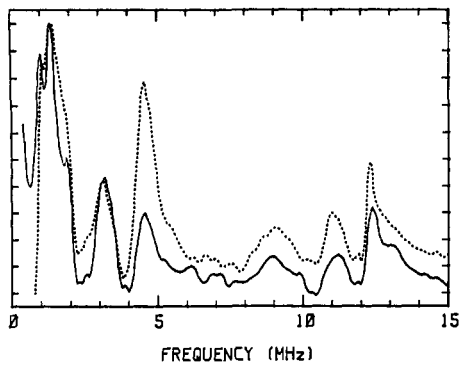

FIGURE 1: Solid line: Three-pulse ESEEM spectrum of Mn·TDH. Sample contained 2.9 mM TDH active sites and 0.77 mM $Mn(OAc)_2$ in 50 mM Tris buffer, pH 8.0, containing 1 mM DTT. The data were acquired at 1.8 K, H = 2900 G, ν = 8.96 GHz (g = 2.2), τ = 162 ns. Dashed line: Three-pulse ESEEM spectrum of Mn·histidine. The data were acquired at 1.8 K, H = 2877 G, ν = 8.86 GHz, and τ = 163 ns.

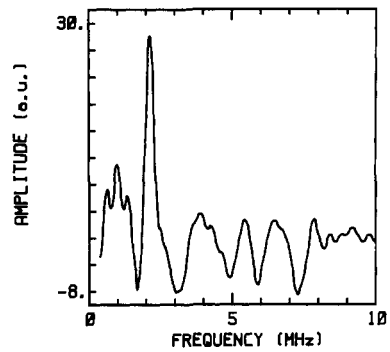

FIGURE 2: Fourier transform of the modulation pattern generated by dividing the three-pulse ESE modulation envelope of Mn·TDH·NAD^+·pyruvate into that of Mn·TDH·NAD^+·[^{2}H]pyruvate. Each sample contained 325 μM TDH active sites, 100 μM $Mn(OAc)_2$, 500 μM deutero- or protiopyruvate, and 150 μM NAD^+ in 100 mM K^+HEPES buffer, pH 8.0. Data were acquired at 1.8 K, H = 3206 G, ν = 8.98 GHz (g = 2), and τ = 220 ns.

Mn·TDH revealed peaks at 1.3, 3.1, 4.6, 9.0, and 11.2 MHz, in addition to the partially suppressed ^{1}H peak seen at 12.4 MHz (Figure 1). Because ^{14}N was the only nucleus with nonzero nuclear spin in this sample (other than ^{1}H, for which a peak appeared at its Larmor frequency) and because the observed peaks did not scale in a simple fashion with the magnetic field (data not shown), it was concluded that the peaks arose from ^{14}N directly coordinated to Mn^{2+}, presumably from protein ligands that contained nitrogen, probably the ϵ-amine of lysine or the imidazole imine nitrogen of histidine.

Ternary complexes of Mn^{2+}, TDH, and NAD^+ yielded ESEEM spectra that were the same as those observed with Mn·TDH. The spectrum of the quaternary complex Mn·TDH·NAD^+·[^{2}H]pyruvate contained a peak at 2.1 MHz, the Larmor frequency of ^{2}H under the experimental conditions, in addition to peaks attributable to ^{14}N. In order to enhance the ^{2}H peak and corroborate its assignment, complexes prepared with unlabeled pyruvate were examined under the same conditions. Spectral subtraction [carried out by division of one modulation envelope into another, followed by Fourier transformation of the quotient (Mims et al., 1984)] of the data for the unlabeled complex from the data for the ^{2}H-labeled complex yielded a spectrum (Figure 2) in which the ^{2}H resonance was clearly resolved. When the Mn·TDH·NAD^+·[^{2}H]pyruvate complex was incubated at room temperature for 1 h before freezing and subsequent data collection, the resulting spectrum contained no detectable ^{2}H resonance.

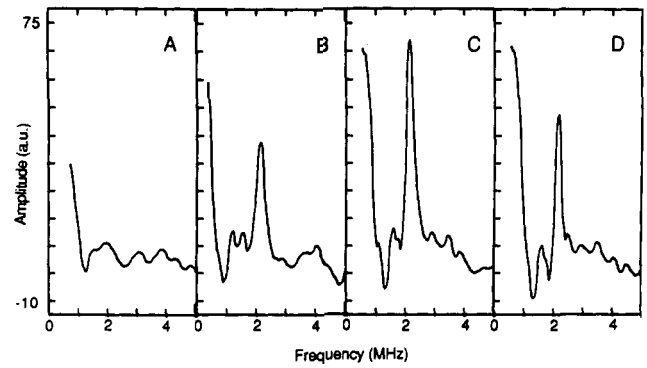

FIGURE 3: Three-pulse ESEEM spectra of MN·TDH·[4-^{2}H]NAD(H) complexes. All samples contained 410 μM TDH, 100 μM $Mn(OAc)_2$, and 210 μM pyridine nucleotide in 100 mM K^+HEPES buffer, pH 8.0. Samples B–D contained 145 μM oxalate in addition to the other components. (A) Mn·TDH·[4-^{2}H]NAD^+. (B) Mn·TDH·[4-^{2}H]-NAD^+·oxalate. (C) Mn·TDH·(*R*-4-^{2}H]NADH·oxalate. (D) Mn·TDH·(*S*)-[4-^{2}H]NADH·oxalate. Data were collected at 1.8 K, H = 3325 G, ν = 9.30 GHz (g = 2), and τ = 212 ns.

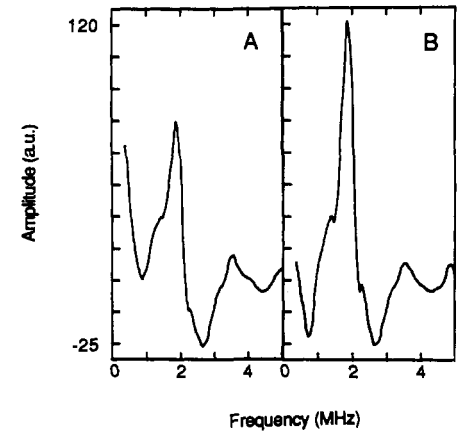

FIGURE 4: Three-pulse ESEEM spectra of Mn·TDH·Cs^+ complexes. (A) 315 μM TDH, 70 μM $Mn(OAc)_2$, 140 μM NAD^+, and 48 mM CsCl in 50 mM Tris buffer, pH 8.0. (B) Same as (A) with the addition of 95 μM oxalate. Data were collected at 1.8 K, H = 3350 G, ν = 9.38 GHz (g = 2), and τ = 210 ns.

Detection of dipolar coupling between ^{2}H and Mn^{2+} was also sought in enzyme complexes in which the ^{2}H label was carried at the 4-position of the nicotinamide ring of the pyridine nucleotide cofactor. The ternary complex Mn·TDH·[4-^{2}H]NAD^+ yielded an ESEEM spectrum in which no ^{2}H signal was apparent. However, upon addition of oxalate, an inhibitor of the catalytic reaction and presumably an analogue of tartrate, the ^{2}H resonance became clearly evident (Figure 3, panels A and B).

The same phenomenon was observed with complexes containing [4-^{2}H]NADH. No ^{2}H signal was evident in ESEEM spectra of Mn·TDH·[4-^{2}H]NADH; however, MN·TDH·[4-^{2}H]NADH·oxalate complexes yielded ESEEM spectra in which the ^{2}H signal was readily apparent (Figure 3, panels C and D). Furthermore, the ^{2}H peak in ESEEM spectra of complexes prepared with (*R*)-[4-^{2}H]NADH was more intense than the signal seen in spectra of complexes containing (*S*)-[4-^{2}H]NADH.

ESEEM spectra of enzyme complexes containing Cs^+ revealed dipolar coupling between Mn^{2+} and ^{133}Cs (Figure 4). The ^{133}Cs Larmor line, which appeared at 1.9 MHz under the experimental conditions, was more intense in spectra of Mn·TDH·Cs^+·NAD^+·oxalate complexes than in spectra of Mn·TDH·Cs^+·NAD^+ complexes.

Model Complexes. ESEEM spectra of several Mn^{2+} model complexes containing nitrogen ligands were obtained for

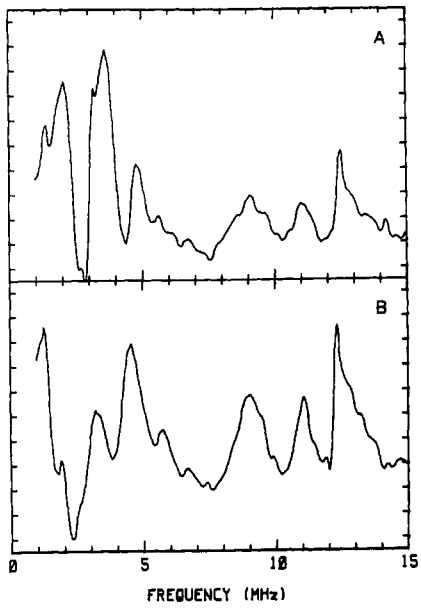

FIGURE 5: (A) Three-pulse ESEEM spectrum of Mn·aspartate. Data were collected at 1.8 K, H = 2915 G, ν = 8.98 GHz (g = 2.2), and τ = 161 ns. (B) Three-pulse ESEEM spectrum of Mn·urocanate. Data were collected at 1.8 K, H = 2870 G, ν = 8.84 GHz (g = 2.2), and τ = 164 ns.

comparison with the spectra of the protein samples. Mn·histidine yielded an ESEEM spectrum similar to that obtained with Mn·TDH (Figure 1), with peaks attributable to ^{14}N at 1.3, 3.1, 4.6, 9.0, and 11.2 MHz. ESEEM spectra of Mn·aspartate and Mn·urocanate contained peaks at 3.5, 4.8, 9, and 11 MHz, as well as some peaks at lower frequencies (Figure 5).

Discussion

Tartrate dehydrogenase requires a divalent metal ion for catalytic activity and shows a strong preference for Mn^{2+} (Tipton & Peisach, 1990; Kohn, et al., 1968). Because Mn^{2+} is paramagnetic, it can serve as a probe of its environment as revealed by ESEEM spectroscopy. The ESEEM phenomenon results from weak magnetic coupling between a paramagnetic center and nuclei with nonzero nuclear spins and is useful for resolution of couplings that are often smaller than the intrinsic line widths obtained in continuous-wave EPR spectra of the same samples (Mims & Peisach, 1981). Under favorable circumstances, substrate and protein ligands to the metal can be characterized by analysis of hyperfine and nuclear quadrupole coupling parameters. Signals arising via dipolar coupling indicate the presence of a species near the metal but not necessarily directly coordinated to it[2] and so can be used to characterize the environment beyond the first coordination sphere of the metal.

In the case of TDH, modulations arising from coupling of ^{14}N to Mn^{2+} were taken as an indication of ligation to Mn^{2+} by an amino acid side chain containing nitrogen and will be discussed below. Unfortunately, a number of factors make it difficult to detect coordination of tartrate or malate to Mn^{2+} directly. TDH follows an ordered kinetic mechanism, with NAD^+ binding after Mn^{2+} but before tartrate or malate (Tipton & Peisach, 1990). Thus, tartrate will not bind to TDH unless NAD^+ is present, in which case catalysis results. This problem can be circumvented by examining dead-end complexes, for example Mn·TDH·NAD^+·pyruvate, or by using tartrate analogues such as oxalate. The question remains, however, what signal to look for. We have not yet successfully detected ^{17}O signals unambiguously, nor have we detected ^{13}C coupling in Mn^{2+} complexes in which the ^{13}C in the ligand would have to couple to Mn^{2+} through an intermediate oxygen atom. For example, we have not detected ^{13}C coupling in Mn^{2+} complexes with [1-^{13}C]pyruvate and [2-^{13}C]pyruvate, although VO^{2+} complexes of ^{13}C-labeled pyruvate yielded ^{13}C isotropic hyperfine couplings in the range of 2–5 MHz (Tipton et al., 1989). Therefore, in our examination of TDH active-site complexes, we have relied upon the detection of dipolar coupling between Mn^{2+} and ^2H on appropriately labeled substrates to infer the proximity of Mn^{2+} to these species. The detection of dipolar coupling to [^2H]pyruvate and [4-^2H]NAD^+ demonstrates that Mn^{2+} does bind in close proximity to the substrates; i.e., Mn^{2+} binds at the active site.

The relatively weak ^2H signal observed in ESEEM spectra of Mn·TDH·NAD^+·[^2H]pyruvate complexes suggested the possibility that, contrary to our expectations, Mn^{2+} and pyruvate were relatively distant from each other. An alternative explanation was that the weak signal arose because the pyruvate methyl deuterons were being exchanged with solvent protons. That the latter was indeed the case was confirmed by the complete loss of the ^2H signal in spectra of Mn·TDH·NAD^+·[^2H]pyruvate complexes that had been incubated for 1 h at room temperature before examination. This exchange reaction is also catalyzed by pigeon liver L-malic enzyme and has been demonstrated in that case to require Mg^{2+} (Bratcher & Hsu, 1982). Presumably, exchange occurs via reversible formation of the pyruvate enolate, a process that would be facilitated by coordination to a divalent metal ion.

Mn^{2+} can be envisioned to perform a number of roles in the catalytic reactions of TDH. Oxidation of the substrate alcohol requires removal of the hydroxyl proton, and coordination of this group to Mn^{2+} would lower the pK by several log units [for example, the pK of Mn-bound water is 10.1 (Reed & Markham, 1984)]. The D-malate and *meso*-tartrate reactions presumably occur via β-keto acid intermediates, and the role of divalent metal ions in catalyzing the decarboxylation of β-keto acids by generating an electron sink through polarization of the ketone carbonyl has long been recognized (Seltzer et al., 1959). Alternatively, Mn^{2+} may be required to orient the substrates properly in the active site. It should be noted that Mn^{2+} could conceivably perform any of these functions with either inner or outer-sphere ligands.

The binding of oxalate to TDH had a pronounced effect on ESEEM spectra of complexes containing [4-^2H]NAD(H). In the absence of oxalate, no Mn–^2H coupling was observed, even though steady-state kinetic data demonstrated that Mn·TDH·NAD^+ and Mn·TDH·NADH complexes form during the catalytic cycle (Tipton & Peisach, 1990). When oxalate was added to these complexes, the ^2H signal became apparent. An explanation consistent with these results is that NAD(H) binding occurs via initial recognition of the adenosine portion

[2] The depth of the modulation of the electron spin echo envelope relative to the amplitude of the electron spin echo envelope transforms into the intensity of the peak in the frequency domain and increases proportionately with the number of nuclei, with the inverse sixth power of the distance between the nucleus and the electron spin, and with the nuclear spin I by the factor $^4/_3I(I + 1)$ (Mims & Peisach, 1981). We cannot yet calculate distances by spectral simulation of dipolar couplings between nuclei and paramagnets with $S > {}^1/_2$ (Mn^{2+} is $S = {}^5/_2$). Therefore, our distance estimates are qualitative. We estimate the upper limit for detection of Mn–^2H dipolar coupling to be 5–5.5 Å, on the basis of data we have collected for Mn·(*R*)-[3-^2H]malate bound in the active site of L-malic enzyme. Model building suggests that the Mn–^2H distance in this complex is 4.5–5.0 Å; the ^2H peak that is found in the frequency domain spectrum has an intensity 3–4 times greater than the baseline noise.

of the cofactor and that the nicotinamide ring has a certain degree of motional freedom until binding of the second substrate locks it into the proper conformation for catalysis. Crystallographic investigations of NADP(H) binding to glutathione reductase have demonstrated that crystals soaked with NADP(H) and analogues of NADP(H) invariably had higher occupancy at the adenine binding site than at the nicotinamide binding site (Pai et al., 1988). These data were interpreted to mean that productive binding of NADP(H) to that enzyme begins with binding of the adenine end of the cofactor. Our data do not, of course, rule out the possibility that a protein conformational change is responsible for bringing Mn^{2+} and NAD(H) together in the active site of TDH.

The intensity of the ^2H signals differed in ESEEM spectra of complexes with (*R*)- and (*S*)-[4-^{2}H]NADH. The more intense signal arising from (*R*)-[4-^{2}H]NADH indicates that the 4*R* deuteron lies closer to Mn^{2+} than the 4*S* deuteron, since the extent of labeling of the two isotopomers is the same. Considering the presumptive role of Mn^{2+} in the catalytic reaction and the nature of the reaction itself, i.e., transfer of a hydride from tartrate (or D-malate) to NAD^+, the most likely arrangement in the active site is one in which the carbon center of tartrate that is being oxidized lies between Mn^{2+} and NAD^+ with its hydroxyl toward Mn^{2+} and the hydrogen toward NAD^+. Thus, the observation that the *pro-R* position of NADH is closer to Mn^{2+} than the *pro-S* position also suggests that hydride delivery occurs to the *re* face of NAD^+. In other words, the ESEEM spectra predict that TDH is an A-side-specific dehydrogenase.[3]

ESEEM spectroscopy offered a convenient means to investigate the monovalent cation requirement of TDH. All the alkali metals have nonzero nuclear spins and are therefore detectable, in principle, by virtue of dipolar coupling to Mn^{2+}. The activation of TDH by monovalent cations has been investigated previously (Tipton & Peisach, 1990; Kohn et al., 1968), and enzyme activity was found to correlate with the ionic radius of the alkali metal, with K^+ supporting maximal activity and larger or smaller cations supporting activity at a lower level. ^{39}K has a small magnetic moment, however, so its low Larmor frequency (about 0.6 MHz under typical experimental conditions) makes it difficult to resolve from the decay of the echo envelope. ^{133}Cs, which has an apparent K_m of 17 mM in the (+)-tartrate oxidation reaction and V_{max} 10% that of K^+ (Tipton & Peisach, 1990), has a larger magnetic moment than ^{39}K and has the further advantage of being an $I = {}^7/_2$ nucleus. Since modulation depth increases with the magnitude of I (Mims & Peisach, 1981), dipolar coupling between Mn^{2+} and ^{133}Cs is readily observed. ESEEM spectra of Mn·TDH·NAD^+ complexes prepared in the presence of 50 mM CsCl, and the absence of any other alkali metals, did reveal dipolar coupling between Mn^{2+} and ^{133}Cs at 1.9 MHz (Figure 4, panel A). The intensity of the Cs signal increased in the presence of oxalate (Figure 4, panel B), indicating either that Cs^+ and Mn^{2+} moved closer together in the presence of oxalate or that oxalate binding increased the concentration of Cs^+ in the vicinity of Mn^{2+}. Although it is difficult to distinguish between these two possibilities, we favor the latter interpretation. In this view, Cs^+ ion pairs with oxalate in the active site and so binds more readily when oxalate is present. An analogous arrangement has been proposed for K^+ and pyruvate in the active site of pyruvate kinase by a number of workers (Muirhead et al., 1986; Lord & Reed, 1987; Tipton et al., 1989). It should be noted that the ESEEM spectra we have obtained do not unequivocally demonstrate that Mn^{2+} is coupled to a single Cs ion; however, the r^{-6} dependence of dipolar interactions insures that distant Cs ions contribute only minimally to the ESE modulation pattern, and the experimental conditions were chosen so that all the Mn^{2+} was bound to the protein. Also, in protein-free samples containing 0.5 mM Mn^{2+} and 50 mM Cs^+, no coupling between Mn^{2+} and Cs^+ was detected; thus, in the protein complexes Cs^+ was certainly concentrated in the vicinity of Mn^{2+}.

The binary Mn·TDH complex was characterized by an ESEEM spectrum containing several peaks that were assigned to ^{14}N (Figure 1) and presumably arose from ligation to Mn^{2+} by lysine or histidine, or perhaps a peptide amide nitrogen. We sought to determine the chemical identity of this ligand (or ligands) by comparison of the TDH ESEEM spectrum with ESEEM spectra of Mn^{2+} model complexes. Although Mn·histidine yielded an ESEEM spectrum that was virtually superimposable on the spectrum of TDH, it did not resolve whether the signals arose from the α-amine nitrogen or the imidazole imine nitrogen, or from both. Complexes that contained only amine nitrogens, for example, Mn·aspartate, and samples such as Mn·urocanate, which has only imine nitrogens available to coordinate to Mn^{2+}, were therefore examined. As shown in Figure 5, these complexes yield very similar ESEEM spectra. In view of the facts that the quadrupole moments of free amine and imine nitrogens are often similar [for example, the quadrupole coupling constants of imidazole and methylamine are 3.3 and 4.0 MHz, respectively (Lucken, 1969)] and the isotopic hyperfine coupling constants of directly coordinated amine and imine nitrogens can be the same or similar,[4] it is not surprising that the ESEEM spectra for directly coordinated amine and imine nitrogens are similar.

Interpretation of the spectra in Figures 1 and 5 must remain qualitative for the present, since the theory for treating modulations in $S > {}^1/_2$ systems is only now being developed. It is clear, however, that transitions between different electron spin manifolds contribute uniquely to the modulation pattern.[5] It should also be noted that the abundance of ^{14}N peaks in Figures 1 and 5 cannot be taken as evidence for coordination by inequivalent nitrogens, although we cannot rule out this possibility, either. Even in an $S = {}^1/_2$ system, because ^{14}N is an $I = 1$ nucleus, up to six $\Delta m_I = 1$ or 2 transitions can occur, leading to six peaks in the frequency spectrum.

Although Mn ESEEM spectra offer little help in identifying nitrogen-containing ligands, we have earlier noted that VO·amine and VO·imine complexes yield distinctive ESEEM spectra (Tipton et al., 1989). We have now examined a number of VO complexes (data not shown) and have found that VO·amine complexes such as $VO(glycinate)_2$ and $VO(ethylenediamine)_2^{2+}$ yield X-band ESEEM spectra at $g = 2$ with peaks at 3.8 and 7.3 MHz, while spectra of VO·imine complexes, such as $VO(imidazole)_4^{2+}$ and $VO(imidazolylacetate)_2$ have broad peaks at 2.5, 5.0, and 8.7 MHz. Thus, when VO^{2+} can be placed in the divalent metal binding site of a protein unambiguously, ESEEM spectroscopy may provide information on the nature of the nitrogen-containing ligands. Unfortunately, in the case of TDH, attempts to prepare a VO^{2+} complex usually resulted in the formation of a mixture of two species, on the basis of continuous-wave EPR spectral analysis.

The results from the ESEEM spectra are summarized and interpreted in Scheme I, which illustrates a possible ar-

[3] Preliminary data based on the analysis of [^{3}H]NADH formed by the TDH-catalyzed oxidation of (2*R*)-[2-^{3}H]malate indicate that this is indeed the case.

[4] Dr. Richard Magliozzo, unpublished results, this laboratory.

[5] Dr. Alan Coffino, unpublished results, this laboratory.

Scheme I

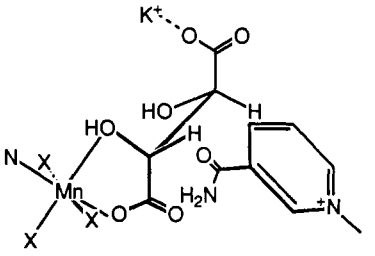

rangement of the substrates in the active site of TDH. Mn^{2+} is shown with one nitrogen-containing ligand, although there may be more than one. We have shown (+)-tartrate as a ligand to Mn^{2+}. Although the ESEEM data do not demonstrate coordination of the substrate to Mn^{2+}, they clearly indicate that Mn^{2+} is in the active site, and the chemical reactions catalyzed by TDH provide a compelling rationale for direct coordination. NAD^+ has been arranged so that the hydride will be transferred to the *re* face of the nicotinamide ring. The monovalent cation is shown coordinated to a substrate carboxyl group, consistent with both spectroscopic and kinetic data which suggest that their binding is interdependent.

Registry No. NAD, 53-84-9; NADH, 58-68-4; TDH, 37250-29-6; Cs, 7440-46-2; Mn, 7439-96-5; pyruvate, 127-17-3; oxalic acid, 144-62-7.

REFERENCES

Attwood, P. V., Tipton, P. A., & Cleland, W. W. (1986) *Biochemistry 25*, 8197–8205.

Bradford, M. M. (1976) *Anal. Biochem. 72*, 248–254.

Bratcher, S. C., & Hsu, R. Y. (1982) *Biochim. Biophys. Acta 702*, 54–60.

Britt, R. D., & Klein, M. P. (1987) *J. Magn. Reson. 74*, 535–540.

Cohn, M., & Townsend, J. (1954) *Nature 173*, 1090–1091.

Kohn, L. D., & Jakoby, W. B. (1968) *J. Biol. Chem. 243*, 2465–2471.

Kohn, L. D., Packman, P. M., Allen, R. H., & Jakoby, W. B. (1968) *J. Biol. Chem. 243*, 2479–2485.

Lin, C. P., Bowman, M. K., & Norris, J. R. (1985) *J. Magn. Reson. 65*, 369–374.

Lord, K. A., & Reed, G. H. (1987) *Inorg. Chem. 26*, 1464–1466.

Lucken, E. A. C. (1969) *Nuclear Quadrupole Coupling Constants*, Chapter 11, Academic Press, New York.

McCracken, J., Peisach, J., & Dooley, D. M. (1987) *J. Am. Chem. Soc. 109*, 4064–4072.

Mims, W. B. (1974) *Rev. Sci. Instrum. 45*, 1583–1591.

Mims, W. B. (1984) *J. Magn. Reson. 59*, 291–306.

Mims, W. B., & Peisach, J. (1981) *Biol. Magn. Reson. 3*, 213–263.

Mims, W. B., Davis, J. L., & Peisach, J. (1984) *Biophys. J. 45*, 755–766.

Muirhead, H., Clayden, D. A., Barford, D., Lorimer, C. G., Fothergill-Gilmore, L. A., Schilz, E., & Schmitt, W. (1986) *EMBO J. 5*, 475–481.

Pai, E. F., Karplus, P. A., & Schulz, G. E. (1988) *Biochemistry 27*, 4465–4474.

Peisach. J., Mims, W. B., & Davis, J. (1979) *J. Biol. Chem. 254*, 12379–12389.

Reed, G. H., & Markham, G. D. (1984) *Biol. Magn. Reson. 6*, 73–142.

Seltzer, S., Hamilton, G. A., & Westheimer, F. H. (1959) *J. Am. Chem. Soc. 81*, 4018–4024.

Tipton, P. A., & Peisach, J. (1990) *Biochemistry 29*, 1749–1759.

Tipton, P. A., McCracken, J., Cornelius, J. B., & Peisach, J. (1989) *Biochemistry 28*, 5720–5728.